



Synthetic Communications

An International Journal for Rapid Communication of Synthetic Organic Chemistry

ISSN: 0039-7911 (Print) 1532-2432 (Online) Journal homepage: <https://www.tandfonline.com/loi/lsyc20>

Synthesis, molecular docking, antimicrobial, antiquorum-sensing and antiproliferative activities of new series of pyrazolo[3,4-*b*]pyridine analogs

Samia S. Hawas, Nadia S. El-Gohary, Moustafa T. Gabr, Mona I. Shaaban & Mahmoud B. El-Ashmawy

To cite this article: Samia S. Hawas, Nadia S. El-Gohary, Moustafa T. Gabr, Mona I. Shaaban & Mahmoud B. El-Ashmawy (2019): Synthesis, molecular docking, antimicrobial, antiquorum-sensing and antiproliferative activities of new series of pyrazolo[3,4-*b*]pyridine analogs, Synthetic Communications, DOI: [10.1080/00397911.2019.1618873](https://doi.org/10.1080/00397911.2019.1618873)

To link to this article: <https://doi.org/10.1080/00397911.2019.1618873>

 View supplementary material 

 Published online: 13 Jul 2019.

 Submit your article to this journal 

 View Crossmark data 



Synthesis, molecular docking, antimicrobial, anti-quorum-sensing and antiproliferative activities of new series of pyrazolo[3,4-*b*]pyridine analogs

Samia S. Hawas^{a,b}, Nadia S. El-Gohary^a, Moustafa T. Gabr^{a,c}, Mona I. Shaaban^d, and Mahmoud B. El-Ashmawy^a

^aDepartment of Medicinal Chemistry, Faculty of Pharmacy, Mansoura University, Mansoura, Egypt;

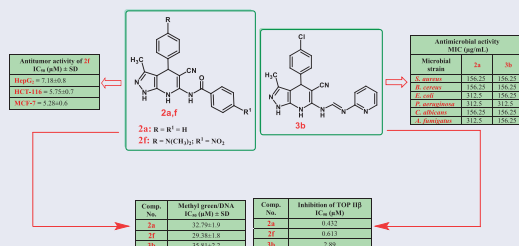
^bDepartment of Pharmaceutical Chemistry, Faculty of Pharmacy, Horus University, New Damietta, Egypt;

^cDepartment of Chemistry, University of Iowa, Iowa City, Iowa, USA; ^dDepartment of Microbiology, Faculty of Pharmacy, Mansoura University, Mansoura, Egypt

ABSTRACT

New series of pyrazolo[3,4-*b*]pyridines were prepared and evaluated for antimicrobial activity toward six selected microorganisms. Compounds **2a**, **3b**, **3d** and **3e** exhibited good activity toward *B. cereus*. On the other hand, **2a** and **3b** evinced interesting activity over *C. albicans*, whereas **2a**, **3b** and **3e** displayed promising activity over *A. fumigatus*. Antiquorum-sensing effectiveness of the new members over *C. violaceum* was also assessed, where compounds **2a** and **3b** exhibited higher activity than that of the reference compound, indole. *In vitro* antiproliferative assessment toward HepG2, HCT-116 and MCF-7 cancer cells evidenced that **2f** has notable effectiveness on all examined cell lines, whereas **3a–c** were active but to a lower extent. *In vivo* antitumor activity of **2f** and **3a–c** against EAC cells was also esteemed, where **2f** and **3c** showed considerable activity comparable to that of doxorubicin. Cytotoxicity screening over WI38 and WISH normal cells evinced that **2f** and **3a–c** are less cytotoxic than doxorubicin. Compounds **2a**, **2f**, **3a–c** and **3e** were evaluated for DNA-binding affinity and topoisomerase II β inhibitory activity. Analogs **2a**, **2f**, **3a** and **3b** illustrated strong DNA-binding affinity, whereas **2a**, **2f** and **3a** exhibited interesting topoisomerase II β inhibitory activity. Compounds **2a** and **2f** were docked into topoisomerase II β , where **2f** showed preferential binding to topoisomerase II β . Computational studies articulated that the new members are in compliance with Veber's standards and Lipinski's rule.

GRAPHICAL ABSTRACT



ARTICLE HISTORY

Received 11 March 2019

KEYWORDS

Pyrazolopyridines; antimicrobial; antiproliferative; DNA-binding; topoisomerase II β ; computational studies

CONTACT Nadia S. El-Gohary  dr.nadiaelgohary@yahoo.com  Department of Medicinal Chemistry, Faculty of Pharmacy, Mansoura University, Mansoura 35516, Egypt.

 Supplemental data for this article is available online at on the [publisher's website](#).

Introduction

The adequate treatment of bacterial, fungal, viral and parasitic infections is prohibited by the development of antimicrobial resistance (AMR). AMR is rising perilously all over the world, and it became a serious public health problem.^[1] Subsequently, new approaches are desired to contend the infection caused by multidrug-resistant microorganisms. Quorum sensing (QS) inhibition is one of such new approaches. QS is a mechanism through which bacterial cells communicate with each other, and it governs diverse processes as biofilm formation and virulence;^[2] consequently, it has turned into a prominent target for new antimicrobial agents. However, antibiotics kill or retard the growth of bacteria, anti-quorum-sensing agents (anti-QS) mitigate bacterial virulence.^[3,4] Thus, the present research is steered toward the synthesis of new antimicrobial agents, and also considered the evolution of new QS inhibitors.

On the other hand, cancer is a leading health hazard, since cancer cells can grow and spread to nearby tissues *via* lymph system or bloodstream. Metastasis is the principal cause of 90% of cancer deaths.^[5] A typical anticancer drug should be cytotoxic to cancer cells without damaging healthy ones. Currently, cancer is a master theme of research, and scientists are inspired in design and invention of new efficacious and selective anticancer agents with various chemical scaffolds, including pyrazolo[3,4-*b*]pyridine nucleus. A variety of antitumor and antimicrobial agents act as DNA minor groove binders.^[6] Likewise, DNA topoisomerases (TOP I, TOP II α and TOP II β) are molecular targets for lots of antibacterial and anticancer drugs.^[7,8] Topoisomerase II (TOP II) plays pivotal roles, including DNA replication and transcription, and hence assuring genomic integrity. The capability to disrupt TOP II and produce enzyme-mediated DNA injury is an efficient approach in cancer therapeutics.^[9]

Pyrazolo[3,4-*b*]pyridine system is a fundamental skeleton in various antidepressant-anxiolytic drugs as cartazolate,^[10] tracazolate^[11] and etazolate^[12] (Figure 1). Additionally, pyrazolo[3,4-*b*]pyridines were proved to possess diverse pharmacological efficacies as antibacterial,^[13–15] antifungal,^[16] antimicrobial^[17–27] and antitumor^[15,17,18,22,24–37] activities. For example, pyrazolo[3,4-*b*]pyridines **A**, **B** and **C**^[32] (Figure 2) were assured to have DNA-binding affinity with distinguished antitumor effectiveness. Also, pyrazolo[3,4-*b*]pyridines **D**, **E** and **F**^[17] (Figure 2) were characterized as DNA-binding agents with interesting antimicrobial and antitumor efficacies.

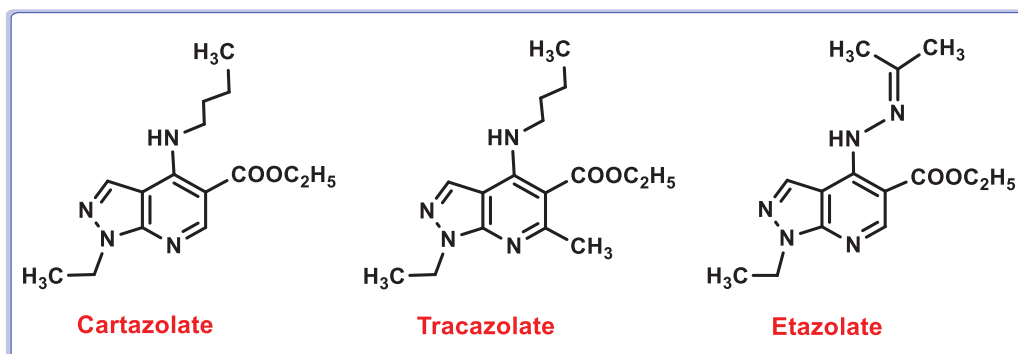


Figure 1. Examples of marketed pyrazolopyridine drugs.

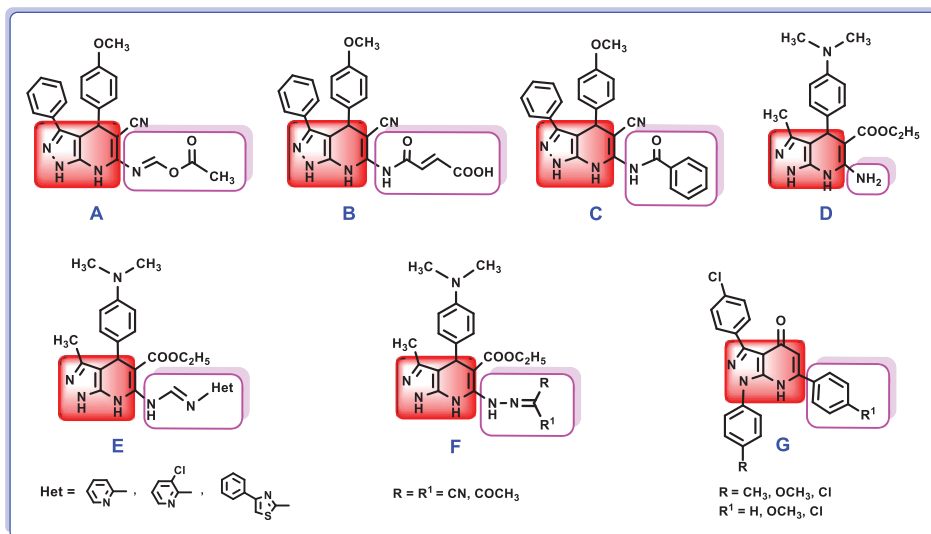


Figure 2. Examples of pyrazolo[3,4-*b*]pyridines with declared DNA-binding affinity (A–F), antitumor (A–G), antimicrobial (D–F) and TOP II inhibitory activities (G).

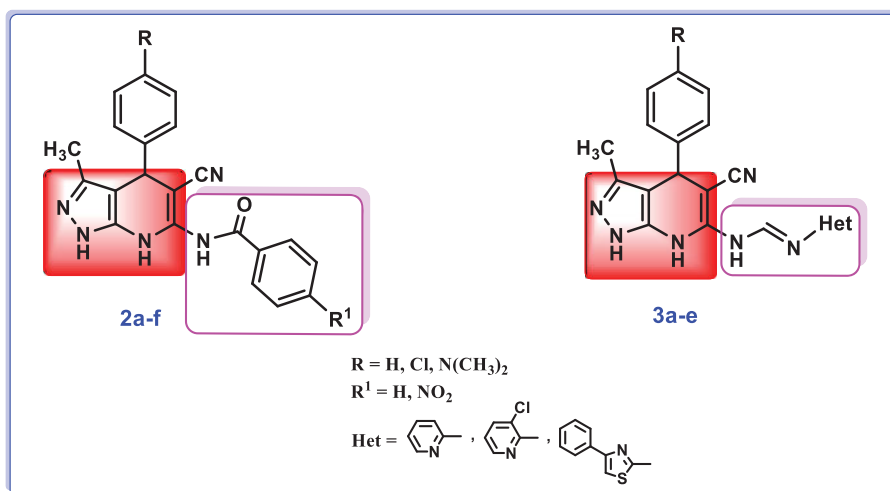


Figure 3. The suggested target compounds carrying (un)substituted benzoylamino 2a-f and *N*-(arylaminomethylene)amino moieties 3a-e.

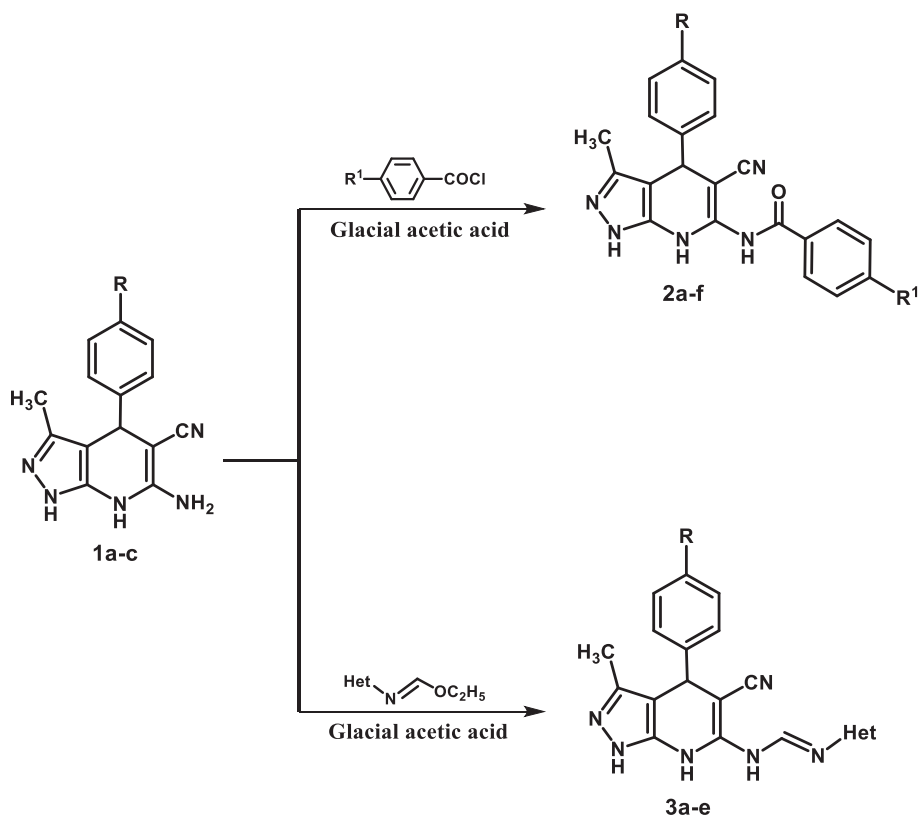
Moreover, pyrazolo[3,4-*b*]pyridines **G**^[36] (Figure 2) were described as TOP II inhibitors with eminent antitumor activity. Motivated by these literature findings and as a continuation to our preceding studies,^[17,18] new series of pyrazolo[3,4-*b*]pyridines carrying (un)substituted benzoylamino 2a-f and *N*-(arylaminomethylene)amino moieties 3a-e (Figure 3) were prepared and evaluated as antimicrobial, anti-QS and anti-proliferative agents. DNA-binding affinity and TOP II β inhibitory activity of 2a, 2f, 3a-c and 3e were assessed to detect their potential mode of action. A thorough study of the structure-activity relationship of the new pyrazolopyridines will flatten the road for design and development of new chemotherapeutic agents.

Results and discussion

Chemistry

The synthetic pathways for the new pyrazolo[3,4-*b*]pyridines **2a-f** and **3a-e** starting with 6-aminopyrazolo[3,4-*b*]pyridine-5-carbonitriles **1a-c**^[37] are illustrated in Scheme 1.

Heating *ortho* aminonitriles **1a-c** with benzoyl chloride or 4-nitrobenzoyl chloride in glacial acetic acid at reflux temperature gave the benzamides **2a-f** in 62-77% yields.



Comp. No.	R	R ¹	Comp. No.	R	Het.
2a	H	H	3a	H	
2b	Cl	H	3b	Cl	
2c	N(CH ₃) ₂	H	3c	N(CH ₃) ₂	
2d	H	NO ₂	3d	N(CH ₃) ₂	
2e	Cl	NO ₂	3e	N(CH ₃) ₂	
2f	N(CH ₃) ₂	NO ₂	-----	-----	-----

Scheme 1. Synthesis of compounds **2a-f** and **3a-e**

Preparation of **3a–e** was accomplished through refluxing **1a–c** with ethyl *N*-(heteroaryl)-formimidates^[38,39] in glacial acetic acid. Spectral and elemental analyses confirmed the structures of the new members.

Biological evaluation

Antimicrobial and antiquorum-sensing screening

The new members, **2a–f** and **3a–e** were evaluated for antimicrobial activity toward Gram-positive bacteria (*Staphylococcus aureus* ATCC 29213 and *Bacillus cereus* UW 85) and Gram-negative bacteria (*Escherichia coli* ATCC 12435 and *Pseudomonas aeruginosa*).^[40–42] Further, antifungal assay over *Candida albicans* (clinical isolate) and *Aspergillus fumigatus* 293 was implemented.^[40,41,43,44] Ampicillin (antibacterial) and fluconazole (antifungal) were employed as reference drugs. Inhibition zone diameters (mm) were measured (Table 1). Minimal inhibitory concentrations (MICs, $\mu\text{g/mL}$ and μM) of **2a**, **2d**, **3b**, **3d** and **3e** (the effective compounds) over the chosen microbial strains were set (Table 2). Results disclosed that **2a** and **3b** have promising activity over

Table 1. Results of antimicrobial and antiquorum-sensing assessment.

Comp. No.	Inhibition zone diameter (mm) ^a						QS inhibition (mm) ^a
	<i>S. aureus</i>	<i>B. cereus</i>	<i>E. coli</i>	<i>P. aeruginosa</i>	<i>C. albicans</i>	<i>A. fumigatus</i>	<i>C. violaceum</i>
2a	19	21	17	17	19	15	19
2b	6	8	–	–	–	–	–
2c	3	2	–	–	–	–	–
2d	16	9	9	7	–	–	–
2e	–	–	–	–	–	–	11
2f	–	–	–	–	–	–	14
3a	–	–	–	–	–	–	–
3b	20	21	19	17	21	23	17
3c	–	–	–	–	–	–	–
3d	17	21	16	11	–	–	–
3e	17	19	–	–	–	19	–
Ampicillin	18	15	23	18	Nd	Nd	Nd
Fluconazole	Nd	Nd	Nd	Nd	11	11	Nd
Indole	Nd	Nd	Nd	Nd	Nd	Nd	15

^aInhibition zone diameter (mm): (–, <2, no activity); (2–9, weak activity); (10–15, moderate activity); (16–25, strong activity); (26–35, very strong activity).

Nd, not defined.

Bold values show the favored data.

Table 2. MICs of the active compounds.

Comp. No.	MIC, $\mu\text{g/mL}$ (μM) ^a					
	<i>S. aureus</i>	<i>B. cereus</i>	<i>E. coli</i>	<i>P. aeruginosa</i>	<i>C. albicans</i>	<i>A. fumigatus</i>
2a	156.25 (611.8)	156.25 (611.8)	312.5 (1223.6)	312.5 (1223.6)	156.25 (611.8)	312.5 (1223.6)
2d	625 (1560.9)	1250 (3121.8)	1250 (3121.8)	1250 (3121.8)	Nd	Nd
3b	156.25 (400.8)	156.25 (400.8)	156.25 (400.8)	312.5 (801.6)	156.25 (400.8)	156.25 (400.8)
3d	312.5 (721.8)	156.25 (360.9)	625 (1443.7)	1250 (2887.4)	Nd	Nd
3e	312.5 (650.25)	156.25 (325.1)	Nd	Nd	Nd	156.25 (325.1)
Ampicillin	78.125 (213.81)	312.5 (855.23)	9.76 (26.71)	156.25 (427.61)	Nd	Nd
Fluconazole	Nd	Nd	Nd	Nd	1250 (4081.35)	2500 (8162.70)

^aMICs (μM) are illustrated between brackets.

Nd, not defined.

Bold values show the favored data.

all tested microorganisms, their activity was two times that of ampicillin over *B. cereus*, eight times that of fluconazole over *C. albicans*, and eight times and sixteen times that of fluconazole over *A. fumigatus* for **2a** and **3b**, respectively. Analogs **3d** and **3e** exhibited good activity on *B. cereus* and considerable activity toward *S. aureus*. On the other hand, **3e** displayed interesting efficacy on *A. fumigatus*. The rest of the screened compounds revealed either weak or no activity toward the selected microorganisms.

Antiquorum-sensing (anti-QS) effectiveness of the same members toward *Chromobacterium violaceum* ATCC 12472 was esteemed,^[40,41,45] and indole was utilized as a comparative agent.

QS system of *C. violaceum* liberates signals that adjust the release of a violet pigment (violacein) that regulates the interspecies cooperative interactions.^[46,47] Consequently, QS inhibition in *C. violaceum* will stop violacein production. Anti-QS efficacy toward *C. violaceum* was estimated: QS inhibition = $(r_2 - r_1)$, (mm), where r_1 is the radius of growth inhibition and r_2 is the overall radius of growth and pigment inhibition. Compounds **2a** and **3b** exhibited strong anti-QS efficacy compared to that of indole, whereas **2e** and **2f** were moderately effective (Table 1).

SAR of analogs 2a-f. The *N*-(4-phenylpyrazolopyridin-6-yl)benzamide **2a** displayed good effectiveness toward Gram-positive bacteria and *C. albicans*, and considerable effectiveness toward Gram-negative bacteria and *A. fumigatus*. Replacing 4-phenyl and/or benzamide in **2a** with 4-(4-chlorophenyl)/4-dimethylaminophenyl and/or 4-nitrobenzamide counterparts led to diminished activity against all screened microorganisms (**2b-f** versus **2a**). On the other hand, the *N*-(4-phenylpyrazolopyridin-6-yl)-4-nitrobenzamide **2d** displayed moderate activity over *S. aureus*, and weak activity toward *B. cereus*, *E. coli* and *P. aeruginosa*. Also, substitution of the phenyl moiety in **2d** with 4-chloro or 4-dimethylamino led to repealed activity toward all screened bacteria and fungi (compounds **2e** and **2f**).

SAR of compounds 3a-e. The 4-(4-chlorophenyl)-6-((pyridin-2-yl)aminomethyleneamino)-pyrazolopyridine analog **3b** showed the highest antimicrobial effectiveness on all tested strains. Replacing 4-(4-chlorophenyl) in **3b** with 4-(unsubstituted phenyl) or 4-(4-(dimethylamino)phenyl) led to diminished activity on all investigated microorganisms (compounds **3a** and **3c**, respectively). Otherwise, exchanging 6-(pyridin-2-yl)aminomethyleneamino substituent in **3c** with 6-(3-chloropyridin-2-yl)aminomethyleneamino led to improved efficacy on the four tested bacteria (compound **3d**), and this might be pertaining to the high lipophilicity of **3d** ($\log P = 2.35$) compared to **3c** ($\log P = 1.73$). On the other hand, exchanging 6-(3-chloropyridin-2-yl)aminomethyleneamino in **3d** with 6-(4-phenylthiazol-2-yl)aminomethyleneamino led to boosted activity over *A. fumigatus*, retained activity over Gram-positive bacteria, and reduced activity over Gram-negative bacteria (compound **3e**).

Antitumor screening

In vitro antiproliferative screening. Antiproliferative effectiveness of the new members was assessed over liver (HepG2), colon (HCT-116) and breast (MCF-7) cancer cells following MTT assay and employing doxorubicin as a positive control.^[48,49] The concentration of compound that prohibits the proliferation of cell viability by 50% (IC_{50} , μM)

Table 3. *In vitro* antiproliferative assay results.

Comp. No.	IC ₅₀ (μM) ^{a,b}		
	HepG2	HCT-116	MCF-7
2a	>100.00	89.16 ± 5.3	87.65 ± 4.7
2b	86.92 ± 4.8	80.28 ± 4.9	77.68 ± 4.3
2c	75.18 ± 4.1	71.39 ± 4.2	62.50 ± 3.7
2d	29.13 ± 2.2	28.37 ± 3.2	20.54 ± 1.6
2e	46.35 ± 2.9	30.27 ± 2.5	31.87 ± 2.1
2f	7.18 ± 0.8	5.75 ± 0.7	5.28 ± 0.6
3a	11.13 ± 1.2	9.38 ± 1.0	12.43 ± 1.5
3b	20.07 ± 2.0	17.89 ± 1.6	16.85 ± 1.5
3c	9.29 ± 1.2	7.96 ± 0.4	8.97 ± 1.0
3d	60.36 ± 4.0	55.78 ± 3.8	48.04 ± 3.5
3e	78.26 ± 4.5	72.91 ± 4.3	68.91 ± 3.8
Doxorubicin	4.50 ± 0.2	5.23 ± 0.3	4.17 ± 0.2

^aIC₅₀ values are the mean ± SD of three readings.

^bIC₅₀ (μM): (1–20, strong activity); (21–50, moderate activity); (51–100, weak activity); (>100, no activity).

Bold values show the favored data.

was set (Table 3). Compound **2f** has notable efficacy toward all chosen cell lines. Likewise, compounds **3a** and **3c** demonstrated interesting effectiveness on all examined cell lines; in addition, **3b** demonstrated considerable activity over the three chosen cancer cells. The other analogs evidenced moderate to weak effect on the examined cancer cells.

SAR of analogs 2a–f. Presence of 4-(unsubstituted phenyl) and 6-(4-nitrobenzoylamino) substituents on the pyrazolopyridine nucleus led to distinguished effectiveness on MCF-7 cells, and feasible effectiveness over HepG2 and HCT-116 cells (analog **2d**). The 4-nitrobenzamide analogs **2d–f** were evinced to be more effective toward all examined cancer cells compared to the unsubstituted benzamide analogs **2a–c**, and this might be ascribed to presence of extra sites of hydrogen bonding in **2d–f**. The *N*-(4-(4-(dimethylamino)phenyl)pyrazolopyridin-6-yl)-4-nitrobenzamide analog **2f** exhibited notable efficacy on the three cancer cells. Replacing 4-(4-(dimethylamino)phenyl) in **2f** with 4-(unsubstituted phenyl) or 4-(4-chlorophenyl) resulted in lower activity on all examined cell lines (compounds **2d** and **2e**), and this might be ascribed to presence of an extra site of hydrogen bonding in **2f**. Contrariwise, replacing 4-(4-chlorophenyl) with 4-(unsubstituted phenyl) led to improved efficacy on all cell lines (**2d** versus **2e**), and this might be pertaining to the reduced lipophilicity of **2d** (logP = 1.96) compared to **2e** (logP = 2.64). The *N*-(4-(4-(dimethylamino)phenyl)pyrazolopyridin-6-yl)benzamide **2c** displayed weak activity on the three cancer cells. Exchanging 4-(4-(dimethylamino)phenyl) substituent in **2c** with 4-(unsubstituted phenyl) or 4-(4-chlorophenyl) led to weakened activity on all cell lines (compounds **2a** and **2b**).

SAR of compounds 3a–e. The 4-(4-(dimethylamino)phenyl)-6-(pyridin-2-yl)aminomethyleneaminopyrazolopyridine analog **3c** showed superior efficacy on all screened cell lines. Replacing 4-(4-(dimethylamino)phenyl) substituent with 4-(unsubstituted phenyl) or 4-(4-chlorophenyl) led to mild decrease in activity over the three cell lines (**3a** and **3b** versus **3c**). On the other hand, replacing 4-(4-chlorophenyl) in **3b** with 4-(unsubstituted phenyl) led to slight improvement in activity toward all inspected cell lines (analog **3a**),

and this might be pertaining to the reduced lipophilicity of **3a** ($\log P = 1.62$) compared to **3b** ($\log P = 2.30$). On contrary, replacing 6-(pyridin-2-yl)aminomethyleneamino substituent in **3c** with 6-(3-chloropyridin-2-yl)aminomethyleneamino or 6-(5-phenylthiazol-2-yl)aminomethyleneamino counterparts gave rise to minimized activity toward all screened cell lines (**3d** and **3e** versus **3c**), and this might be pertaining to the increased lipophilicity of **3d** and **3e** ($\log P = 2.35$ and 3.35 , respectively) compared to **3c** ($\log P = 1.73$). The activity of compounds **3a**, **3b**, **3d** and **3e** is relying on the compound's lipophilicity, the decrease in lipophilicity led to improvement in activity, the order of activity is **3a** > **3b** > **3d** > **3e**.

In vivo antitumor screening. Compounds **2f** and **3a–c** (with significant *in vitro* antiproliferative activity) were screened for *in vivo* antitumor efficacy toward Ehrlich ascites carcinoma (EAC) in mice,^[50–52] and doxorubicin was utilized as a comparative drug. Mean survival time (MST) and % increase in lifespan (%ILS) of mice injected with EAC were set (Table 4), where **2f** and **3c** exhibited the greatest activity. Tumor size parameters were esteemed (Table 5), where **2f** and **3c** demonstrated a marked reduction in tumor volume and tumor cell count. Hemoglobin (Hb), red blood cells (RBCs) and white blood cells (WBCs) count were estimated (Table 6), where **2f** and **3c** manifested higher Hb and RBCs levels and lower WBCs count than doxorubicin.

In vitro cytotoxicity screening against normal cell lines. *In vitro* cytotoxicity of **2f** and **3a–c** over lung fibroblast (WI38) and amnion epithelial (WISH) normal cells^[48,49] was assessed. IC_{50} values (μM) of the investigated analogs were calculated (Table 7).

Table 4. Effect of **2f** and **3a–c** on MST and % ILS of mice bearing EAC.

Group	MST (day) ^a	% ILS
Normal	Nd	Nd
EAC only	16.0	Nd
2f	48.0	200.00
3a	30.0	87.50
3b	33.0	106.25
3c	51.0	216.75
Doxorubicin	57.0	256.25

^aResults are the mean of three readings.

Nd, not defined.

Bold values show the favored data.

Table 5. Effect of **2f** and **3a–c** on tumor size parameters of mice bearing EAC.

Group	Tumor volume (mL) ^a	Viable tumor cell count ($10^6/mL$) ^a
Normal	Nd	Nd
EAC only	9.60	72.76
2f	2.70	21.49
3a	4.60	32.28
3b	4.00	30.78
3c	2.40	19.60
Doxorubicin	2.00	15.25

^aResults are the mean of three readings.

Nd, not defined.

Bold values show the favored data.

Table 6. Effect of **2f** and **3a-c** on hematological count of mice bearing EAC.

Group	Hb (g/dl) ^a	RBCs (10 ⁶ /mm ³) ^a	WBCs (10 ³ /mm ³) ^a
Normal	13.16	6.14	5.49
EAC only	7.86	3.57	20.25
2f	12.31	5.58	8.66
3a	10.95	5.05	13.64
3b	11.27	5.18	10.68
3c	12.49	5.67	8.62
Doxorubicin	12.25	5.56	8.79

^aResults are the mean of three readings.

Bold values show the favored data.

Table 7. Cytotoxicity of **2f** and **3a-c** against WI38 and WISH normal cells.

Comp. No.	IC ₅₀ (μM) ^{a,b}	
	WI38	WISH
2f	46.85 ± 2.7	39.27 ± 2.5
3a	35.42 ± 2.0	28.96 ± 1.9
3b	52.91 ± 2.9	37.11 ± 2.3
3c	61.60 ± 3.4	45.92 ± 2.8
Doxorubicin	6.68 ± 0.5	8.14 ± 0.9

^aIC₅₀ values are the mean ± SD of three readings.

^bIC₅₀ (μM): (1–20, strong activity); (21–50, moderate activity); (51–100, weak activity); (>100, no cytotoxicity).

The four analogs showed lower cytotoxicity than doxorubicin (standard drug), and they were proved to be safe against the tested normal cell lines at their cytotoxic concentrations over the selected cancer cells.

Mechanistic study

DNA-binding assay. DNA-binding interaction is the mode of action of diverse antimicrobial and anticancer agents,^[6] pyrazolo[3,4-*b*]pyridines are amongst these agents.^[17,18,32] Pyrazolo[3,4-*b*]pyridine ring is isosteric to purine, and its derivatives might contest with purines and prohibit DNA synthesis. Accordingly, methyl green/DNA displacement assay^[53] was embraced to assess the potentiality of the efficacious compounds to bind to DNA.

Methyl green/DNA displacement assay is a colorimetric method^[53] for estimation of the displacement of methyl green from DNA by agents with DNA-binding affinity. Concentrations of **2a**, **2f**, **3a-c**, **3e**, and doxorubicin (DNA-binding agent) that reduce absorbance of methyl green/DNA complex by 50% (IC₅₀, μM) were set (Table 8). Results indicated that **2a**, **2f**, **3a** and **3b** have strong binding affinity analogous to that of doxorubicin, whereas **3c** and **3e** displayed moderate affinity. The six members are predicted to act *via* binding to DNA.

Topoisomerase IIβ inhibition assay. DNA topoisomerase II (TOP II) is a prime target for certain antibacterial and anticancer agents.^[7,8] Quinolones are vastly utilized antibiotics that inhibit DNA gyrase (bacterial form of TOP II),^[54] and they are studied as anticancer agents.^[55,56] It is believed that TOP II might be the prime target for the new

Table 8. DNA-binding testing results.

Comp. No.	IC ₅₀ (μM) ^a
2a	32.79 ± 1.9
2f	29.38 ± 1.8
3a	35.43 ± 2.3
3b	35.81 ± 2.2
3c	41.42 ± 2.5
3e	51.26 ± 3.0
Doxorubicin	31.27 ± 1.8

^aIC₅₀ values are the mean ± SD of three readings.

Bold values show the favored data.

Table 9. Results of topoisomerase IIβ inhibition.

Comp. No.	IC ₅₀ (μM) ^a
2a	0.432
2f	0.613
3a	0.933
3b	2.89
3c	1.96
3e	3.15
Doxorubicin	0.727

^aIC₅₀ values are the mean of three readings.

Bold values show the favored data.

pyrazolopyridines which are structurally related to the well-known class of quinolone antibiotics. Thus, TOP IIβ inhibitory activity of the most effective antimicrobial and/or antitumor pyrazolopyridines **2a**, **2f**, **3a–c** and **3e** was evaluated,^[57] and compared to that of doxorubicin (positive control). Results (Table 9) indicated that analogs **2a**, **2f** and **3a** have the highest efficacy in the enzymatic assay.

Computational studies

Molecular docking

For the sake of getting an insight into the binding mode of compounds **2a** and **2f** to TOP IIβ, a molecular docking study relied on the crystal structure of TOP IIβ in complex with DNA and etoposide (PDB code: 3QX3, <https://www.rcsb.org/3d-view/3QX3/1>) was accomplished. The two investigated compounds **2a** and **2f** possessed estimated binding energy to TOP IIβ of −18.1 and −19.7 kcal/mol, respectively, in comparison to doxorubicin that revealed binding energy of −20.6 kcal/mol. 3D Interactions of **2a** (one of the most active compounds in the antimicrobial screening) and **2f** (the most active compound in the antitumor screening) with TOP IIβ binding site were generated by Molegro 2.5 software^[58] and they are shown in Figures 4A and 5A, respectively. The itemized analyses of the binding interactions of **2a** and **2f** to TOP IIβ are displayed in their 2D binding modes (generated by Lead IT 2.3.2 software^[59]) featuring key hydrogen bonding interactions with Asp479 residue (Figures 4B and 5B, respectively) similarly to the binding pose of etoposide to TOP IIβ. The 2D binding modes of etoposide and doxorubicin to TOP IIβ are shown in Figure 6A,B, respectively.

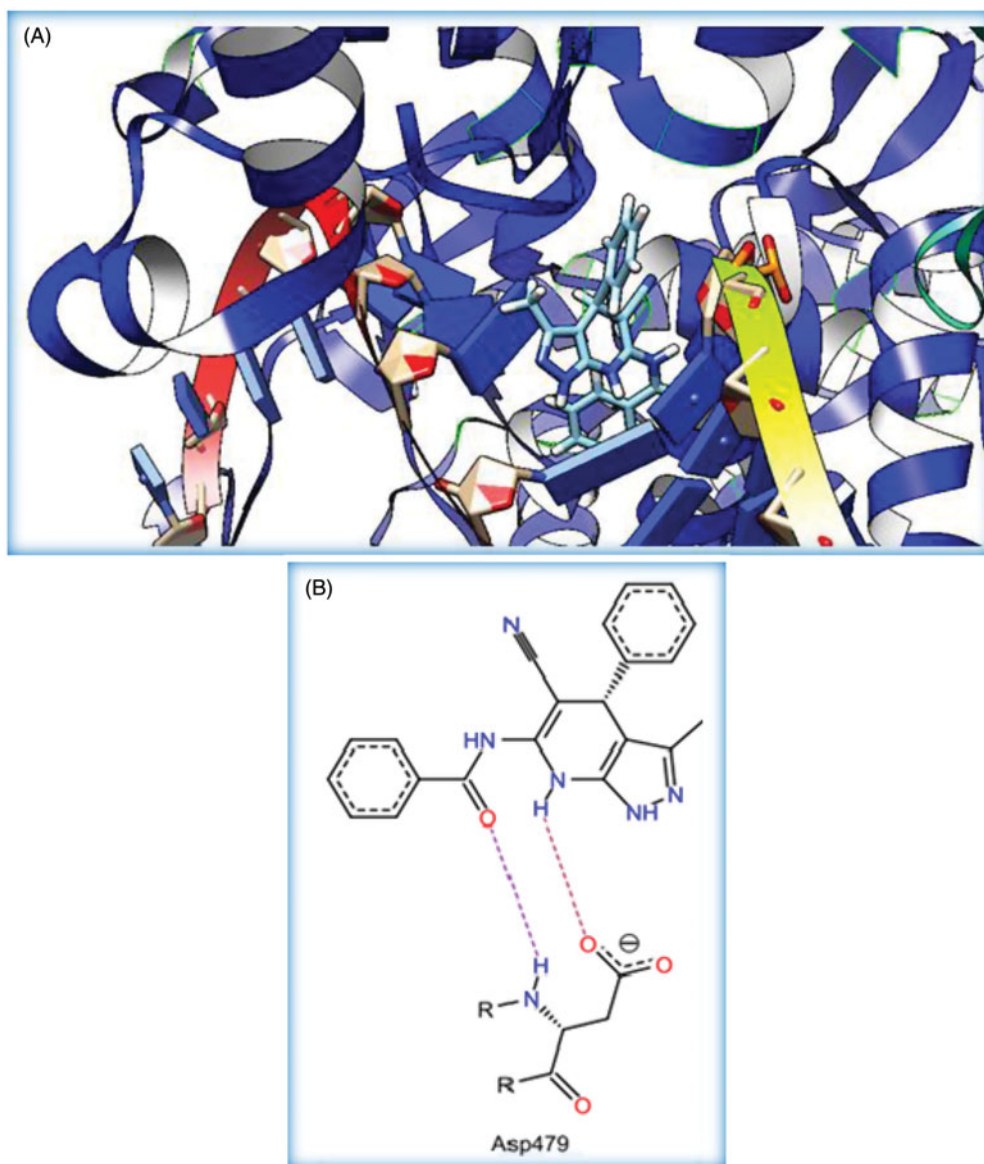


Figure 4. (A) 3D Interaction of **2a** with TOP $II\beta$ binding site. The atoms are colored as follows: blue for nitrogen atoms, red for oxygen atoms, white for hydrogen atoms and cyan for carbon atoms. (B) 2D Interaction of **2a** with TOP $II\beta$ binding site. Dashed lines show hydrogen bonds.

3D and 2D pharmacophoric maps of the structural features of **2a** (Supplementary Figure S1A,B) and **2f** (Figure 7A,B) were established using LigandScout 4.1 software.^[60] The exact pharmacophoric features include hydrogen bond acceptors and donors as directed vectors along with lipophilic areas which are expressed by spheres. The overlay of pharmacophoric map of **2f** to pharmacophoric map of the binding of etoposide to TOP $II\beta$ revealed satisfactory alignment (Figure 7C). These results come in good agreement with the results of *in vitro* antiproliferative screening which demonstrated that **2f**

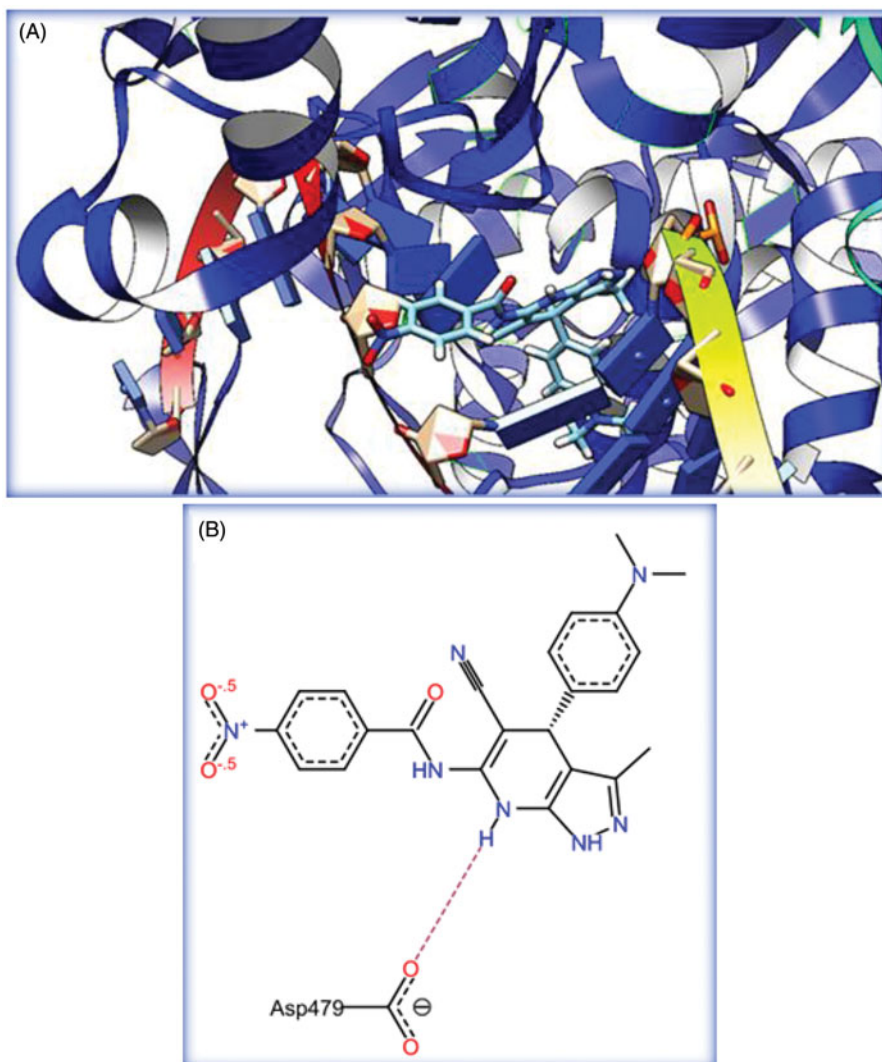


Figure 5. (A) 3D Interaction of **2f** with TOP $II\beta$ binding site. The atoms are colored as follows: blue for nitrogen atoms, red for oxygen atoms, white for hydrogen atoms and cyan for carbon atoms. (B) 2D Interaction of **2f** with TOP $II\beta$ binding site. Dashed lines show hydrogen bonds.

is the most active analog in this study against the three opted cancer cell lines (Table 3). The overlay of pharmacophoric map of **2a** to pharmacophoric map of the binding of etoposide to TOP $II\beta$ is shown in Supplementary Figure S1C. Ultimately, molecular docking studies revealed a preliminary conception of the binding mode of the new analogs.

Molinspiration, preadmet and molsoft calculations

Computational analyses are helpful in the speculation of physicochemical properties, pharmacokinetics, and toxicity of compounds.^[61] Consequently, the new members were

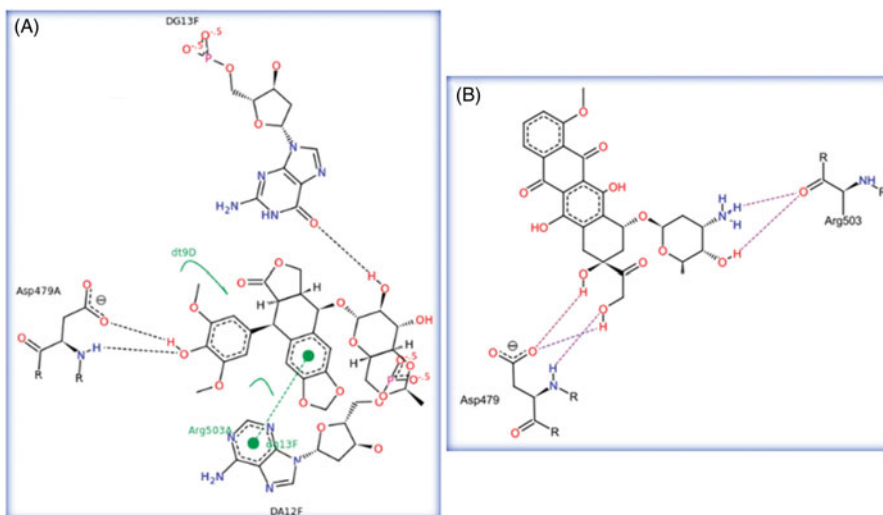


Figure 6. (A) 2D Interaction of etoposide with TOP II β binding site. (B) 2D Interaction of doxorubicin with TOP II β binding site. Dashed lines show hydrogen bonds.

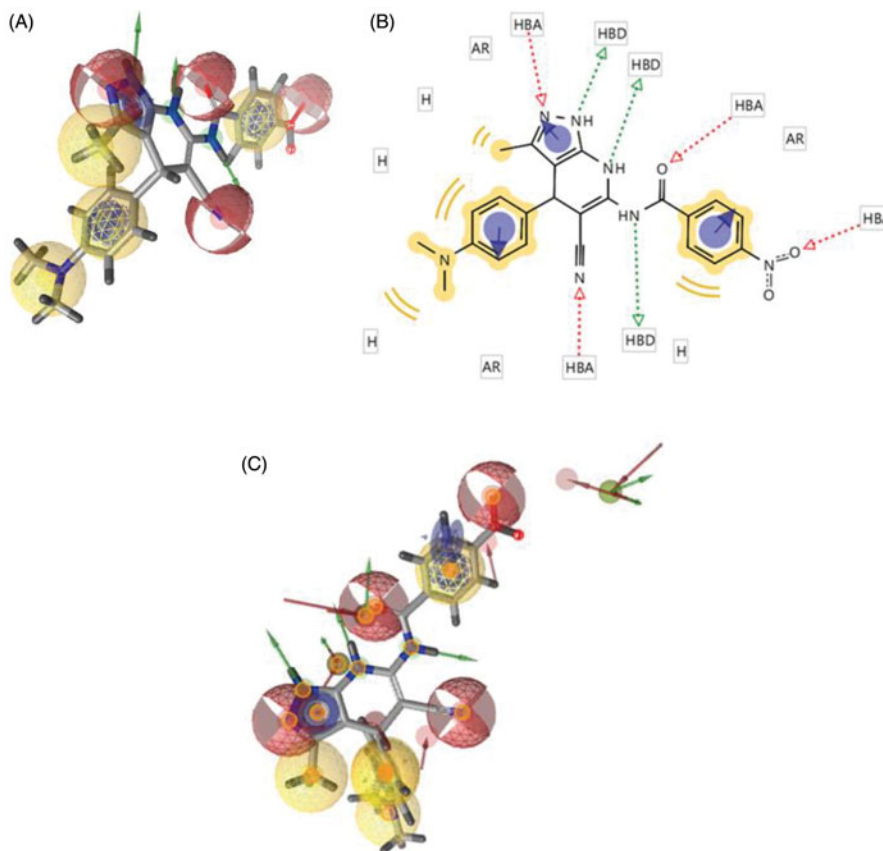


Figure 7. (A) 3D Pharmacophoric map of 2f; pharmacophore color coding is yellow for hydrophobic regions, red for hydrogen acceptors and green for hydrogen donors. (B) 2D Pharmacophoric map of 2f; H is hydrophobic center, AR is aryl, HBA is hydrogen bond acceptor and HBD is hydrogen bond donor. (C) The overlay of pharmacophoric map of 2f to pharmacophoric map of the binding of etoposide to TOP II β .

studied for the prediction of Lipinski's rule^[62,63] and Veber's standards.^[63,64] As well, their carcinogenicity^[65] and drug score values^[66] were prophesied. Results are discussed in the supplemental data.

Conclusion

Results of antimicrobial testing proved that **2a** and **3b** have interesting efficacy over all examined microorganisms as well as strong QS inhibitory activity. Consequently, **2a** and **3b** might be regarded as efficacious antimicrobial agents with reduced danger of AMR. Turning into results of *in vitro* antiproliferative testing, **2f** displayed the greatest effectiveness on the three screened cell lines; moreover, **3c** manifested explicit activity on the three cell lines. As well, analogs **2f** and **3c** evinced excellent *in vivo* antitumor effectiveness over EAC cells, and they were evidenced to be safe against both normal cells at their cytotoxic concentrations over the tested cancer cells. Results of DNA-binding and TOP II β assays revealed that **2a**, **2f**, **3a** and **3b** have strong DNA-binding affinity, whereas **2a**, **2f** and **3a** exhibited interesting TOP II β inhibitory activity. Collectively referred, **2a** is regarded as an efficacious antimicrobial agent with powerful DNA-binding affinity and TOP II β inhibitory activity. As well, **2f** and **3c** are considered as efficacious and selective antiproliferative agents through targeting DNA and TOP II β . Further, docking studies fostered the efficient binding interactions of **2a** and **2f** to TOP II β . Computational studies clarified that all of the checked compounds are in conformity with Veber's and Lipinski's rule standards, and they are thought to display interesting oral absorption. The full attained results corroborated that rational design of the new analogs as antimicrobial and antiproliferative agents was competent, and the efficacious members in the present research will be subjugated to extra structural amendments to get new more efficacious derivatives.

Experimental

All melting points ($^{\circ}\text{C}$) were measured using Stuart melting point apparatus SMP30. Unicam SP 1000 IR spectrometer (ν in cm^{-1}) was employed for recording IR spectra (KBr disc). ^1H and ^{13}C -NMR spectral analyses were accomplished on Bruker 500 MHz spectrometer using $\text{DMSO}-d_6$ as solvent. Mass spectrometer (JEOL JMS-600H, 70 eV) was utilized to record mass spectra. Elemental analyses (% C, H, N) were performed, and they were in congruence with the proposed structures. TLC, silica gel plates 60 F254 were used to monitor reaction times, and UV (366, 245 nm) was employed for visualization of the spots. Elution was done utilizing chloroform/methanol (9:1). *Ortho* aminonitriles **1a-c**^[37] and ethyl *N*-(heteroaryl)formimidates^[38,39] were prepared following the published procedures.

Chemistry

Synthesis of benzamide analogs 2a-f

A mixture of **1a-c** (0.002 mol) and benzoyl chloride (0.281 g, 0.002 mol) or 4-nitrobenzoyl chloride (0.371 g, 0.002 mol) was refluxed in glacial acetic acid (10 mL) for 8–15 h.

The solution was concentrated and the solid obtained was filtered and crystallized from ethanol/water (2:1) to produce **2a-f**.

***N*-(5-Cyano-3-methyl-4-phenyl-4,7-dihydro-1H-pyrazolo[3,4-*b*]pyridin-6-yl)benzamide (2a)**

Yield 75%, *m.p.* 130–132 °C. IR: 3405, 3278 (3NH), 2210 (C≡N), 1652 (C=O). ¹H-NMR δ: 2.03 (s, 3H, CH₃), 4.15 (s, 1H, C₄-H), 5.92 (s, 1H, NH), 7.09–7.95 (m, 11H, Ar-H, NH), 11.35 (s, 1H, NH). ¹³C-NMR δ: 10.0, 29.8, 55.8, 103.4, 115.2, 126.0, 127.8, 128.4, 128.8, 129.7, 133.0, 136.2, 137.8, 145.7, 160.1, 161.8, 173.6. MS *m/z* (%): 357 (0.68, M⁺+2), 356 (0.63, M⁺+1), 355 (0.79, M⁺), 57 (100.00). Anal. Calcd (Found) for C₂₁H₁₇N₅O (355.40): C, 70.97 (70.67); H, 4.82 (4.61); N, 19.71 (19.46) %.

***N*-(4-(4-Chlorophenyl)-5-cyano-3-methyl-4,7-dihydro-1H-pyrazolo[3,4-*b*]pyridin-6-yl)benzamide (2b)**

Yield 62%, *m.p.* 155–156 °C. IR: 3372, 3311, 3169 (3NH), 2191 (C≡N), 1648 (C=O). ¹H-NMR δ: 2.28 (s, 3H, CH₃), 4.28 (s, 1H, C₄-H), 5.89 (s, 1H, NH), 7.47 (s, 1H, NH), 7.48–7.51 (m, 4H, Ar-H), 7.59–7.63 (m, 2H, Ar-H), 7.93–7.95 (m, 3H, Ar-H), 9.35 (s, 1H, NH). ¹³C-NMR δ: 9.9, 33.8, 79.7, 104.2, 116.3, 127.7, 128.5, 128.7, 129.2, 130.2, 130.7, 132.8, 133.9, 134.7, 158.6, 160.9, 167.3. MS *m/z* (%): 389 (0.99, M⁺-1), 269 (100.00). Anal. Calcd (Found) for C₂₁H₁₆ClN₅O (389.84): C, 64.70 (64.47); H, 4.14 (4.32); N, 17.96 (17.62) %.

***N*-(5-Cyano-4-(4-(dimethylamino)phenyl)-3-methyl-4,7-dihydro-1H-pyrazolo[3,4-*b*]pyridin-6-yl)benzamide (2c)**

Yield 70%, *m.p.* 268–269 °C. IR: 3483, 3423, 3384 (3NH), 2205 (C≡N), 1685 (C=O). ¹H-NMR δ: 2.07 (s, 3H, CH₃), 3.10 (s, 6H, N(CH₃)₂), 4.46 (s, 1H, C₄-H), 7.29 (s, 1H, NH), 7.41 (d, 2H, Ar-H, *J* = 7.5 Hz), 7.50 (t, 2H, Ar-H, *J* = 8.0 Hz), 7.60 (d, 2H, Ar-H, *J* = 7.5 Hz), 7.65 (t, 1H, Ar-H, *J* = 7.5 Hz), 7.79 (s, 1H, NH), 7.81 (s, 1H, NH), 7.93 (d, 2H, Ar-H, *J* = 7.5 Hz). ¹³C-NMR δ: 12.1, 24.3, 41.9, 79.7, 116.4, 118.5, 123.5, 123.7, 125.0, 128.7, 130.8, 133.9, 134.7, 136.4, 150.0, 158.6, 160.9, 165.8. MS *m/z* (%): 396 (0.78, M⁺-2), 105 (100.00). Anal. Calcd (Found) for C₂₃H₂₂N₆O (398.47): C, 69.33 (69.17); H, 5.57 (5.89); N, 21.09 (21.31) %.

***N*-(5-Cyano-3-methyl-4-phenyl-4,7-dihydro-1H-pyrazolo[3,4-*b*]pyridin-6-yl)-4-nitrobenzamide (2d)**

Yield 76%, *m.p.* 135–136 °C. IR: 3406 (3NH), 2265 (C≡N), 1694 (C=O). ¹H-NMR δ: 2.03 (s, 3H, CH₃), 2.93 (s, 2H, 2NH), 4.11 (s, 1H, NH), 4.45 (s, 1H, C₄-H), 7.09–7.34 (m, 5H, Ar-H), 8.15 (d, 2H, Ar-H, *J* = 8.0 Hz), 8.30 (d, 2H, Ar-H, *J* = 8.0 Hz). ¹³C-NMR δ: 10.2, 36.2, 55.9, 102.9, 117.9, 123.7, 125.7, 127.3, 128.1, 130.7, 136.5, 136.8, 144.9, 149.9, 159.3, 165.9, 173.2. MS *m/z* (%): 402 (0.18, M⁺+2), 401 (0.12, M⁺+1), 400

(0.13, M^+), 185 (100.00). Anal. Calcd (Found) for $C_{21}H_{16}N_6O_3$ (400.40): C, 63.00 (63.32); H, 4.03 (4.29); N, 20.99 (20.66) %.

***N*-(4-(4-Chlorophenyl)-5-cyano-3-methyl-4,7-dihydro-1H-pyrazolo[3,4-*b*]pyridin-6-yl)-4-nitrobenzamide (2e)**

Yield 77%, *m.p.* 180–182 °C. 1H -NMR δ : 2.10 (s, 3H, CH_3), 4.62 (s, 1H, C_4 -H), 7.46 (s, 1H, NH), 7.50 (d, 2H, Ar-H, $J=7.0$ Hz), 7.60 (d, 2H, Ar-H, $J=7.0$ Hz), 8.16 (d, 2H, Ar-H, $J=6.5$ Hz), 8.19 (s, 1H, NH), 8.31 (d, 2H, Ar-H, $J=7.0$ Hz), 10.55 (s, 1H, NH). ^{13}C -NMR δ : 12.1, 24.3, 79.7, 116.4, 118.5, 123.8, 125.0, 128.7, 130.3, 130.7, 134.7, 136.4, 141.9, 150.0, 158.6, 160.9, 165.8. MS *m/z* (%): 436 (0.3, M^++1), 435 (0.31, M^+), 434 (0.41, M^+-1), 57 (100.00). Anal. Calcd (Found) for $C_{21}H_{15}ClN_6O_3$ (434.84): C, 58.01 (57.76); H, 3.48 (3.16); N, 19.33 (19.64) %.

***N*-(5-Cyano-4-(4-(dimethylamino)phenyl)-3-methyl-4,7-dihydro-1H-pyrazolo[3,4-*b*]pyridin-6-yl)-4-nitrobenzamide (2f)**

Yield 67%, *m.p.* 295–296 °C. IR: 3406, 3420, 3363 (3NH), 2206 ($C\equiv N$), 1693 ($C=O$). 1H -NMR δ : 2.07 (s, 3H, CH_3), 3.03 (s, 6H, $N(CH_3)_2$), 4.38 (s, 1H, C_4 -H), 7.10 (d, 2H, Ar-H, $J=6.5$ Hz), 7.35 (d, 2H, Ar-H, $J=7.5$ Hz), 7.70 (d, 2H, Ar-H, $J=7.5$ Hz), 7.96 (d, 2H, Ar-H, $J=7.5$ Hz), 8.36 (s, 1H, NH), 8.42 (s, 1H, NH), 8.75 (s, 1H, NH). ^{13}C -NMR δ : 10.6, 30.1, 42.2, 75.0, 106.4, 118.7, 123.8, 130.6, 131.2, 131.9, 132.1, 133.4, 133.9, 148.4, 148.9, 158.4, 189.9. Anal. Calcd (Found) for $C_{23}H_{21}N_7O_3$ (443.47): C, 62.29 (62.08); H, 4.77 (4.49); N, 22.11 (22.43) %.

***Synthesis of N*-(5-cyano-3-methyl-4-(un)substituted phenyl)-4,7-dihydro-1H-pyrazolo[3,4-*b*]pyridin-6-yl)-*N'*-(heteroaryl)formamidines 3a-e**

A mixture of **1a–c** (0.002 mol) and ethyl *N*-(heteroaryl)formimidate (0.002 mol) in glacial acetic acid (10 mL) was refluxed for 16–24 h. The solution was cooled and the solid obtained was filtered and crystallized from acetic acid to give **3a–e**.

***N*-(5-Cyano-3-methyl-4-phenyl-4,7-dihydro-1H-pyrazolo[3,4-*b*]pyridin-6-yl)-*N'*-(pyridin-2-yl)formamidine (3a)**

Yield 70%, *m.p.* 145–146 °C. IR: 3426 (3NH), 2199 ($C\equiv N$). 1H -NMR δ : 2.02 (s, 3H, CH_3), 3.82 (s, 1H, NH), 4.11 (s, 1H, C_4 -H), 5.85 (s, 1H, NH), 6.41 (s, 1H, NH), 7.22–7.30 (m, 9H, Ar-H), 7.87 (s, 1H, $CH=N$). ^{13}C -NMR δ : 10.2, 36.2, 55.7, 102.9, 107.9, 111.8, 125.7, 127.3, 128.1, 128.2, 136.3, 136.9, 144.9, 147.6, 159.3, 159.7, 161.9, 173.2. MS *m/z* (%): 357 (0.89, M^++2), 356 (0.84, M^++1), 355 (0.96, M^+), 185 (100.00). Anal. Calcd (Found) for $C_{20}H_{17}N_7$ (355.41): C, 67.59 (67.27); H, 4.82 (4.97); N, 27.59 (27.78) %.

***N*-(4-(4-Chlorophenyl)-5-cyano-3-methyl-4,7-dihydro-1H-pyrazolo[3,4-*b*]pyridin-6-yl)-*N'*-(pyridin-2-yl)formamidine (3b)**

Yield 73%, *m.p.* 140–141 °C. IR: 3380, 3206 (3NH), 2207 (C≡N). ¹H-NMR δ: 2.06 (s, 3H, CH₃), 4.79 (s, 1H, C₄-H), 5.84 (s, 1H, NH), 6.39–6.41 (m, 2H, Ar-H), 7.10 (d, 2H, Ar-H, *J* = 8.0 Hz), 7.25 (d, 2H, Ar-H, *J* = 8.5 Hz), 7.22 (s, 1H, NH), 7.30–7.34 (m, 2H, Ar-H), 7.87 (s, 1H, CH = N), 11.33 (s, 1H, NH). ¹³C-NMR δ: 10.4, 32.2, 79.7, 103.9, 108.0, 111.8, 116.4, 127.6, 129.4, 130.0, 137.0, 139.7, 142.4, 147.5, 158.6, 159.7, 160.9, 172.1. MS *m/z* (%): 390 (0.19, M⁺), 389 (0.17, M⁺-1), 57 (100.00). Anal. Calcd (Found) for C₂₀H₁₆ClN₇ (389.85): C, 61.62 (61.33); H, 4.14 (4.42); N, 25.15 (25.27) %.

***N*-(5-Cyano-4-(4-(dimethylamino)phenyl)-3-methyl-4,7-dihydro-1H-pyrazolo[3,4-*b*]pyridin-6-yl)-*N'*-(pyridin-2-yl)formamidine (3c)**

Yield 66%, *m.p.* 165–166 °C. IR: 3423 (3NH), 2205 (C≡N). ¹H-NMR δ: 1.97 (s, 3H, CH₃), 2.98 (s, 6H, N(CH₃)₂), 4.02 (s, 1H, C₄-H), 5.88 (s, 1H, NH), 6.40 (d, 1H, Ar-H, *J* = 8.0 Hz), 6.59 (d, 2H, Ar-H, *J* = 8.5 Hz), 7.09 (d, 2H, Ar-H, *J* = 8.5 Hz), 7.31–7.35 (t, 1H, Ar-H, *J* = 8.5 Hz), 7.67 (d, 1H, Ar-H, *J* = 8.5 Hz), 7.82–7.87 (m, 1H, Ar-H), 8.04 (s, 1H, CH = N), 9.65 (s, 1H, NH), 11.20 (s, 1H, NH). ¹³C-NMR δ: 10.2, 35.2, 41.9, 68.6, 103.9, 108.0, 111.8, 112.5, 119.6, 127.7, 129.6, 133.6, 137.0, 147.5, 148.8, 154.4, 158.9, 159.7, 173.4. MS *m/z* (%): 396 (1.0, M⁺-2), 57 (100.00). Anal. Calcd (Found) for C₂₂H₂₂N₈ (398.47): C, 66.31 (66.62); H, 5.57 (5.31); N, 28.12 (27.83) %.

***N*-(5-Cyano-4-(4-(dimethylamino)phenyl)-3-methyl-4,7-dihydro-1H-pyrazolo[3,4-*b*]pyridin-6-yl)-*N'*-(3-chloropyridin-2-yl)formamidine (3d)**

Yield 69%, *m.p.* 295–296 °C. IR: 3422 (3NH), 2205 (C≡N). ¹H-NMR δ: 1.89 (s, 3H, CH₃), 3.03 (s, 6H, N(CH₃)₂), 4.88 (s, 1H, C₄-H), 6.58 (d, 2H, Ar-H, *J* = 8.5 Hz), 7.16 (d, 2H, Ar-H, *J* = 8.5 Hz), 7.62–7.75 (m, 3H, Ar-H), 8.20 (s, 1H, CH = N), 10.57 (s, 1H, NH), 12.12 (s, 2H, 2NH). ¹³C-NMR δ: 9.8, 36.6, 41.1, 56.3, 97.4, 111.2, 112.4, 119.9, 121.9, 128.1, 129.6, 136.5, 136.7, 146.2, 149.6, 155.6, 156.2, 163.5, 165.9. MS *m/z* (%): 435 (0.13, M⁺+2), 434 (0.30, M⁺+1), 433 (2.52, M⁺), 57 (100.00). Anal. Calcd (Found) for C₂₂H₂₁ClN₈ (432.92): C, 61.04 (61.37); H, 4.89 (4.66); N, 25.88 (25.51) %.

***N*-(5-Cyano-4-(4-(dimethylamino)phenyl)-3-methyl-4,7-dihydro-1H-pyrazolo[3,4-*b*]pyridin-6-yl)-*N'*-(4-phenylthiazol-2-yl)formamidine (3e)**

Yield 77%, *m.p.* 151–153 °C. IR: 3420 (3NH), 2209 (C≡N). ¹H-NMR δ: 1.92 (s, 3H, CH₃), 2.86 (s, 6H, N(CH₃)₂), 4.01 (s, 1H, C₄-H), 6.59 (d, 2H, Ar-H, *J* = 8.5 Hz), 7.03 (s, 1H, Thiazole-H), 7.07 (d, 2H, Ar-H, *J* = 8.5 Hz), 7.29–7.51 (m, 5H, Ar-H), 7.70 (s, 1H, CH = N), 8.02 (s, 1H, NH), 8.09 (s, 1H, NH), 8.95 (s, 1H, NH). ¹³C-NMR δ: 10.8, 35.8, 40.4, 80.3, 101.9, 104.0, 108.4, 112.9, 116.8, 117.8, 126.1, 128.2, 129.2, 129.8, 130.8, 149.3, 150.4, 159.1, 160.3, 161.5, 172.6. MS *m/z* (%): 482 (0.42, M⁺+1), 481 (0.87, M⁺), 269 (100.00). Anal. Calcd (Found) for C₂₆H₂₄N₈S (480.59): C, 64.98 (64.73); H, 5.03 (5.31); N, 23.32 (23.11) %.

Biology

Full biological assay methods are presented in the supplemental data.

Antimicrobial and anti-quorum-sensing evaluation

Antibacterial assay^[40–42]

Antifungal assay^[40,41,43,44]

Antiquorum-sensing assay^[40,41,45]

Antitumor evaluation

In vitro antiproliferative assay^[48,49]

In vivo antitumor assay^[50–52]

Cytotoxicity assay^[48,49]

Mechanistic study

DNA-binding assay^[53]

Topoisomerase II β assay^[57]

Supporting information

Results of computational studies, full experimental details, IR, ¹H-NMR, ¹³C-NMR and mass spectra are described in the supplemental data.

Acknowledgments

Appreciation to Holding Company for Biological Products and Vaccines (VACSERA), Egypt, for accomplishing the *in vitro* antiproliferative, *in vivo* antitumor, cytotoxicity, and topoisomerase II β assays.

References

- [1] Sekyere, J. O.; Asante, J. Emerging Mechanisms of Antimicrobial Resistance in Bacteria and Fungi: Advances in the Era of Genomics. *Future Microbiol.* **2018**, *13*, 241–262. DOI: [10.2217/fmb-2017-0172](https://doi.org/10.2217/fmb-2017-0172).
- [2] Abisado, R. G.; Benomar, S.; Klaus, J. R.; Dandekar, A. A.; Chandler, J. R. Bacterial Quorum Sensing, and Microbial Community Interactions. *mBio.* **2018**, *9*, 1–13. DOI: [10.1128/mBio.01749-18](https://doi.org/10.1128/mBio.01749-18).
- [3] Haque, D. S.; Ahmad, F.; Dar, S. A.; Jawed, A.; Mandal, R. K.; Wahid, M.; Lohani, M.; Khan, S.; Singh, V.; Akhter, N. Developments in Strategies for Quorum Sensing Virulence Factor Inhibition to Combat Bacterial Drug Resistance. *Microb. Pathog.* **2018**, *121*, 293–302. DOI: [10.1016/j.micpath.2018.05.046](https://doi.org/10.1016/j.micpath.2018.05.046).
- [4] Gerdt, J. P.; Blackwell, H. E. Competition Studies Confirm Two Major Barriers That Can Preclude the Spread of Resistance to Quorum-Sensing Inhibitors in Bacteria. *ACS Chem. Biol.* **2014**, *9*, 2291–2299. DOI: [10.1021/cb5004288](https://doi.org/10.1021/cb5004288).

- [5] Chaffer, C. L.; Weinberg, R. A. A Perspective on Cancer Cell Metastasis. *Science* **2011**, *331*, 1559–1564. DOI: [10.1126/science.1203543](https://doi.org/10.1126/science.1203543).
- [6] Baraldi, P. G.; Bovero, A.; Fruttarolo, F.; Preti, D.; Tabrizi, M. A.; Pavani, M. G.; Romagnoli, R. DNA Minor Groove Binders as Potential Antitumor and Antimicrobial Agents. *Med. Res. Rev.* **2004**, *24*, 475–528.
- [7] Kathiravan, M. K.; Khilare, M. M.; Nikoomanesh, K.; Chothe, A. S.; Jain, K. S. Topoisomerase as Target for Antibacterial and Anticancer Drug Discovery. *J. Enzyme Inhib. Med. Chem.* **2013**, *28*, 419–435. DOI: [10.3109/14756366.2012.658785](https://doi.org/10.3109/14756366.2012.658785).
- [8] Pommier, Y.; Leo, E.; Zhang, H.; Marchand, C. DNA Topoisomerases and Their Poisoning by Anticancer and Antibacterial Drugs. *Chem. Biol.* **2010**, *17*, 421–433. DOI: [10.1016/j.chembiol.2010.04.012](https://doi.org/10.1016/j.chembiol.2010.04.012).
- [9] Nitiss, J. L. Targeting DNA Topoisomerase II in Cancer Chemotherapy. *Nat. Rev. Cancer* **2009**, *9*, 338–350. DOI: [10.1038/nrc2607](https://doi.org/10.1038/nrc2607).
- [10] Kripalani, K. J.; Dreyfuss, J.; Nemeč, J.; Cohen, A. I.; Meeker, F.; Egli, P. Biotransformation in the Monkey of Cartazolate (SQ 65,396), a Substituted Pyrazolopyridine Having Anxiolytic Activity. *Xenobiotica* **1981**, *11*, 481–488. DOI: [10.3109/00498258109045858](https://doi.org/10.3109/00498258109045858).
- [11] Thompson, S. A.; Wingrove, P. B.; Connelly, L.; Whiting, P. J.; Wafford, K. A. Tracazolate Reveals a Novel Type of Allosteric Interaction with Recombinant Gamma-Aminobutyric Acid(A) Receptors. *Mol. Pharmacol.* **2002**, *61*, 861–869. DOI: [10.1124/mol.61.4.861](https://doi.org/10.1124/mol.61.4.861).
- [12] Marcade, M.; Bourdin, J.; Loiseau, N.; Peillon, H.; Rayer, A.; Drouin, D.; Schweighoffer, F.; Désiré, L. Etazolate, a Neuroprotective Drug Linking GABA(A) Receptor Pharmacology to Amyloid Precursor Protein Processing. *J. Neurochem.* **2008**, *106*, 392–404. DOI: [10.1111/j.1471-4159.2008.05396.x](https://doi.org/10.1111/j.1471-4159.2008.05396.x).
- [13] Mohamed, H. S. H.; Gad, M.N.M.; El-Zanaty, A. M.; Ahmed, S. A. Synthesis, Characterization and Antibacterial Activities of Novel Thieno, Pyrazol Pyridines and Pyrazolopyrimidine Derivatives. *Der Pharma Chem.* **2018**, *10* (5), 121–127.
- [14] Maqbool, T.; Nazeer, A.; Khan, M. N.; Elliott, M. C.; Khan, M. A.; Ashraf, M.; Nasrullah, M.; Arshad, S.; Munawar, M. A. Pyrazolopyridines II: Synthesis and Antibacterial Screening of 6-Aryl-3-Methyl-1-Phenyl-1*H*-Pyrazolo[3,4-*b*]Pyridine-4-Carboxylic Acids. *Asian J. Chem.* **2014**, *26*, 2870–2872. DOI: [10.14233/ajchem.2014.15918](https://doi.org/10.14233/ajchem.2014.15918).
- [15] Hamama, W. S.; El-Gohary, H. G.; Soliman, M.; Zoorob, H. H. A Versatile Synthesis, PM3-Semiempirical, Antibacterial, and Antitumor Evaluation of Some Bioactive Pyrazoles. *J. Heterocyclic Chem.* **2012**, *49*, 543–554. DOI: [10.1002/jhet.806](https://doi.org/10.1002/jhet.806).
- [16] Quiroga, J.; Villarreal, Y.; Gálvez, J.; Ortíz, A.; Insuasty, B.; Abonia, R.; Raimondi, M.; Zaccchino, S. Synthesis and Antifungal *in Vitro* Evaluation of Pyrazolo[3,4-*b*]Pyridines Derivatives Obtained by aza-Diels-Alder Reaction and Microwave Irradiation. *Chem. Pharm. Bull.* **2017**, *65*, 143–150. DOI: [10.1248/cpb.c16-00652](https://doi.org/10.1248/cpb.c16-00652).
- [17] El-Gohary, N. S.; Shaaban, M. I. Design, Synthesis, Antimicrobial, Antiquorum-Sensing and Antitumor Evaluation of New Series of Pyrazolopyridine Derivatives. *Eur. J. Med. Chem.* **2018**, *157*, 729–742. DOI: [10.1016/j.ejmech.2018.08.008](https://doi.org/10.1016/j.ejmech.2018.08.008).
- [18] El-Gohary, N. S.; Shaaban, M. I. New Pyrazolopyridine Analogs: Synthesis, Antimicrobial, Antiquorum-Sensing and Antitumor Screening. *Eur. J. Med. Chem.* **2018**, *152*, 126–136. DOI: [10.1016/j.ejmech.2018.04.025](https://doi.org/10.1016/j.ejmech.2018.04.025).
- [19] Hamza, A.; El-Sayed, H. A.; Assy, M. G.; Ouf, N. H.; Farhan, M. E. Synthesis and Antimicrobial Activity of Some New Triazine, 1,3-Oxazine, Fused Pyridine and Pyrimidine Derivatives. *World Appl. Sci. J.* **2018**, *36*, 637–645.
- [20] Abdel-Mohsen, S. A.; El-Emary, T. I. New Pyrazolo[3,4-*b*]Pyridines: Synthesis and Antimicrobial Activity. *Der Pharma Chem.* **2018**, *10* (4), 44–51.
- [21] Samar, C.; Ismail, A.; Helmi, T.; Khiari, J.; Bassem, J. Substituted Pyrazolo[3,4-*b*]Pyridin-3-ones and Pyrazolo[3,4-*b*]Pyridine-5-Carbaldehyde, New One-Pot Synthesis Strategy Amelioration Using Vinamidinium Salts, Antibacterial and Antifungal Activities Promising Environmental Protection. *J. Bacteriol. Parasitol.* **2017**, *8*, 1–8. DOI: [10.4172/2155-9597.1000310](https://doi.org/10.4172/2155-9597.1000310).

- [22] Salem, M. S.; Ali, M. A. M. Novel Pyrazolo[3,4-*b*]Pyridine Derivatives: Synthesis, Characterization, Antimicrobial and Antiproliferative Profile. *Biol. Pharm. Bull.* **2016**, *39*, 473–483. DOI: [10.1248/bpb.b15-00586](https://doi.org/10.1248/bpb.b15-00586).
- [23] Sindhu, J.; Singh, H.; Khurana, J. M.; Bhardwaj, J. K.; Saraf, P.; Sharma, C. Synthesis and Biological Evaluation of Some Functionalized 1*H*-1,2,3-Triazole Tethered Pyrazolo[3,4-*b*]Pyridin-6(7*H*)-Ones as Antimicrobial and Apoptosis Inducing Agents. *Med. Chem. Res.* **2016**, *25*, 1813–1830. DOI: [10.1007/s00044-016-1604-0](https://doi.org/10.1007/s00044-016-1604-0).
- [24] Hafez, H. N.; El-Gazzar, A. R. B. A. Synthesis of Pyranopyrazolo *N*-Glycoside and Pyrazolopyranopyrimidine *C*-Glycoside Derivatives as Promising Antitumor and Antimicrobial Agents. *Acta Pharm.* **2015**, *65*, 215–233. DOI: [10.1515/acph-2015-0022](https://doi.org/10.1515/acph-2015-0022).
- [25] Nagender, P.; Malla, R. G.; Naresh, K. R.; Poornachandra, Y.; Ganesh, K. C.; Narsaiah, B. Synthesis, Cytotoxicity, Antimicrobial and anti-Biofilm Activities of Novel Pyrazolo[3,4-*b*]Pyridine and Pyrimidine Functionalized 1,2,3-Triazole Derivatives. *Bioorg. Med. Chem. Lett.* **2014**, *24*, 2905–2908. DOI: [10.1016/j.bmcl.2014.04.084](https://doi.org/10.1016/j.bmcl.2014.04.084).
- [26] El-Borai, M. A.; Rizk, H. F.; Abd-Aal, M. F.; El-Deeb, I. Y. Synthesis of Pyrazolo[3,4-*b*]Pyridines under Microwave Irradiation in Multi-Component Reactions and Their Antitumor and Antimicrobial activities-Part 1. *Eur. J. Med. Chem.* **2012**, *48*, 92–96. DOI: [10.1016/j.ejmech.2011.11.038](https://doi.org/10.1016/j.ejmech.2011.11.038).
- [27] El-Borai, M. A.; Rizk, H. F.; Beltagy, D. M.; El-Deeb, I. Y. Microwave-Assisted Synthesis of Some New Pyrazolopyridines and Their Antioxidant, Antitumor and Antimicrobial Activities. *Eur. J. Med. Chem.* **2013**, *66*, 415–422. DOI: [10.1016/j.ejmech.2013.04.043](https://doi.org/10.1016/j.ejmech.2013.04.043).
- [28] El-Borai, M. A.; Awad, M. K.; Rizk, H. F.; Atlam, F. M. Design, Synthesis and Docking Study of Novel Imidazolyl Pyrazolopyridine Derivatives as Antitumor Agents Targeting MCF7. *Curr. Org. Synth.* **2018**, *15*, 275–285. DOI: [10.2174/1570179414666170512125759](https://doi.org/10.2174/1570179414666170512125759).
- [29] Metwally, N. H.; Deeb, E. A. Synthesis, Anticancer Assessment on Human Breast, Liver and Colon Carcinoma Cell Lines and Molecular Modeling Study Using Novel Pyrazolo[4,3-*c*]Pyridine Derivatives. *Bioorg. Chem.* **2018**, *77*, 203–214. DOI: [10.1016/j.bioorg.2017.12.032](https://doi.org/10.1016/j.bioorg.2017.12.032).
- [30] Rao, H. S. P.; Adigopula, L. N.; Ramadas, K. One-Pot Synthesis of Densely Substituted Pyrazolo[3,4-*b*]-4,7-Dihydropyridines. *ACS Comb. Sci.* **2017**, *19*, 279–285. DOI: [10.1021/acscombsci.6b00156](https://doi.org/10.1021/acscombsci.6b00156).
- [31] Nagender, P.; Kumar, R. N.; Reddy, G. M.; Swaroop, D. K.; Poornachandra, Y.; Kumar, C. G.; Narsaiah, B. Synthesis of Novel Hydrazone and Azole Functionalized Pyrazolo[3,4-*b*]Pyridine Derivatives as Promising Anticancer Agents. *Bioorg. Med. Chem. Lett.* **2016**, *26*, 4427–4432. DOI: [10.1016/j.bmcl.2016.08.006](https://doi.org/10.1016/j.bmcl.2016.08.006).
- [32] Eissa, I. H.; El-Naggar, A. M.; El-Hashash, M. A. Design, Synthesis, Molecular Modeling and Biological Evaluation of Novel 1*H*-Pyrazolo[3,4-*b*]Pyridine Derivatives as Potential Anticancer Agents. *Bioorg. Chem.* **2016**, *67*, 43–56. DOI: [10.1016/j.bioorg.2016.05.006](https://doi.org/10.1016/j.bioorg.2016.05.006).
- [33] Zhao, B.; Li, Y.; Xu, P.; Dai, Y.; Luo, C.; Sun, Y.; Ai, J.; Geng, M.; Duan, W. Discovery of Substituted 1*H*-Pyrazolo[3,4-*b*]Pyridine Derivatives as Potent and Selective FGFR Kinase Inhibitors. *ACS Med. Chem. Lett.* **2016**, *7*, 629–634. DOI: [10.1021/acsmchemlett.6b00066](https://doi.org/10.1021/acsmchemlett.6b00066).
- [34] Fathy, U.; Younis, A.; Awad, H. M. Ultrasonic Assisted Synthesis, Anticancer and Antioxidant Activity of Some Novel Pyrazolo[3,4-*b*]Pyridine Derivatives. *J. Chem. Pharm. Res.* **2015**, *7*, 4–12.
- [35] Elneairy, M. A. A.; Eldine, S. M.; Mohamed, A. S. I. Novel Fused Thienopyridine and Pyrazolopyridine Derivatives: Synthesis, Characterization and Cytotoxicity. *Der Pharma Chem.* **2015**, *7* (5), 284–295.
- [36] Tabrizi, M. A.; Baraldi, P. G.; Baraldi, S.; Prencipe, F.; Preti, D.; Saponaro, G.; Romagnoli, R.; Gessi, S.; Merighi, S.; Stefanelli, A.; et al. Synthesis and Biological Evaluation of Pyrazolo[3,4-*b*]Pyridin-4-Ones as a New Class of Topoisomerase II Inhibitors. *Med. Chem.* **2015**, *11*, 342–353.
- [37] Mohamed, N. R.; Khaireldin, N. Y.; Fahmy, A. F.; El-Sayed, A. A. Facile Synthesis of Fused Nitrogen Containing Heterocycles as Anticancer Agents. *Der Pharma Chem.* **2010**, *2* (1), 400–417.

- [38] Binobaid, A.; Iglesias, M.; Beetstra, D. J.; Kariuki, B.; Dervisi, A.; Fallis, I. A.; Cavell, K. J. Expanded Ring and Functionalised Expanded Ring *N*-Heterocyclic Carbenes as Ligands in Catalysis. *Dalton Trans.* **2009**, 0 (35), 7099–7112. DOI: [10.1039/b909834h](https://doi.org/10.1039/b909834h).
- [39] Leeming, M. R. G.; Penrose, A. B. Triazapentadienes Useful as Miticides. *Ger. Offen.* **1977**, DE 2717280 A1 19771110.
- [40] El-Gohary, N. S.; Shaaban, M. I. Antimicrobial and Antiquorum-Sensing Studies. Part 3: Synthesis and Biological Evaluation of New Series of [1,3,4]Thiadiazole and Fused [1,3,4]Thiadiazole Derivatives. *Arch. Pharm. Chem. Life. Sci.* **2015**, 348, 283–297. DOI: [10.1002/ardp.201400381](https://doi.org/10.1002/ardp.201400381).
- [41] El-Gohary, N. S.; Shaaban, M. I. Synthesis, Antimicrobial, Antiquorum-Sensing, and Cytotoxic Activities of New Series of Isoindoline-1,3-Dione, Pyrazolo[5,1-*a*]Isoindole and Pyridine Derivatives. *Arch. Pharm. Chem. Life. Sci.* **2015**, 348, 666–680. DOI: [10.1002/ardp.201500037](https://doi.org/10.1002/ardp.201500037).
- [42] Clinical Laboratory Standards Institute (CLSI). *Performance Standards for Antimicrobial Susceptibility Testing; Twenty-Fifth Informational Supplement*. Clinical and Laboratory Standards Institute: Wayne, PA, USA, **2015**; M100–S25.
- [43] Clinical Laboratory Standards Institute (CLSI). *Reference Method for Broth Dilution Antifungal Susceptibility Testing of Yeasts; Approved Standard*, 3rd ed. Clinical and Laboratory Standards Institute: Wayne, PA, USA, **2008**; M27–A3.
- [44] Clinical Laboratory Standards Institute (CLSI). *Reference Method for Broth Dilution Antifungal Susceptibility Testing of Filamentous Fungi; Approved Standard*, 2nd ed. Clinical and Laboratory Standards Institute: Wayne, PA, USA, **2008**; M38–A2.
- [45] McClean, K. H.; Winson, M. K.; Fish, L.; Taylor, A.; Chhabra, S. R.; Camara, M.; Daykin, M.; Lamb, J. H.; Swift, S.; Bycroft, B. W.; et al. Quorum Sensing and *Chromobacterium violaceum*: Exploitation of Violacein Production and Inhibition for the Detection of *N*-Acyl Homoserine Lactones. *Microbiology* **1997**, 143, 3703–3711. DOI: [10.1099/00221287-143-12-3703](https://doi.org/10.1099/00221287-143-12-3703).
- [46] Morohoshi, T.; Kato, M.; Fukamachi, K.; Kato, N.; Ikeda, T. *N*-Acylhomoserine Lactone Regulates Violacein Production in *Chromobacterium violaceum* Type Strain ATCC 12472. *FEMS Microbiol. Lett.* **2008**, 279, 124–130. DOI: [10.1111/j.1574-6968.2007.01016.x](https://doi.org/10.1111/j.1574-6968.2007.01016.x).
- [47] Devescovi, G.; Kojic, M.; Covaceuszach, S.; Cámara, M.; Williams, P.; Bertani, I.; Subramoni, S.; Venturi, V. Negative Regulation of Violacein Biosynthesis in *Chromobacterium violaceum*. *Front. Microbiol.* **2017**, 8, 1–11. <https://doi.org/10.3389/fmicb.2017.00349>
- [48] Denizot, F.; Lang, R. Rapid Colorimetric Assay for Cell Growth and Survival. Modifications to the Tetrazolium Dye Procedure Giving Improved Sensitivity and Reliability. *J. Immunol. Methods* **1986**, 89, 271–277. DOI: [10.1016/0022-1759\(86\)90368-6](https://doi.org/10.1016/0022-1759(86)90368-6).
- [49] Gerlier, D.; Thomasset, T. Use of MTT Colorimetric Assay to Measure Cell Activation. *J. Immunol. Methods* **1986**, 94, 57–63.
- [50] Oberling, C.; Guerin, M. The Role of Viruses in the Production of Cancer. *Adv. Cancer Res.* **1954**, 2, 353–423.
- [51] Sheeja, K. R.; Kuttan, G.; Kuttan, R. Cytotoxic and Antitumour Activity of Berberine. *Amala Res. Bull.* **1997**, 17, 73–76.
- [52] Clarkson, B. D.; Burchenal, J. H. Preliminary Screening of Antineoplastic Drugs. *Prog. Clin. Cancer* **1965**, 1, 625–629.
- [53] Burren, N. S.; Frigo, A.; Rasmussen, R. R.; McAlpine, J. B. A Colorimetric Microassay for the Detection of Agents That Interact with DNA. *J. Nat. Prod.* **1992**, 55, 1582–1587.
- [54] Collin, F.; Karkare, S.; Maxwell, A. Exploiting Bacterial DNA Gyrase as a Drug Target: Current State and Perspectives. *Appl. Microbiol. Biotechnol.* **2011**, 92, 479–497. DOI: [10.1007/s00253-011-3557-z](https://doi.org/10.1007/s00253-011-3557-z).
- [55] Chou, L. C.; Chen, C. T.; Lee, J. C.; Way, T. D.; Huang, C. H.; Huang, S. M.; Teng, C. M.; Yamori, T.; Wu, T. S.; Sun, C. M.; et al. Synthesis and Preclinical Evaluations of 2-(2-Fluorophenyl)-6,7-Methylenedioxyquinolin-4-one Monosodium Phosphate (CHM-1-P-Na)

- as a Potent Antitumor Agent. *J. Med. Chem.* **2010**, *53*, 1616–1629. DOI: [10.1021/jm901292j](https://doi.org/10.1021/jm901292j).
- [56] Larsen, A. K.; Escargueil, A. E.; Skladanowski, A. Catalytic Topoisomerase II Inhibitors in Cancer Therapy. *Pharmacol. Ther.* **2003**, *99*, 167–181.
- [57] Smith, N. A.; Byl, J. A.; Mercer, S. L.; Dewese, J. E.; Osheroff, N. Etoposide Quinone Is a Covalent Poison of Human Topoisomerase II β . *Biochemistry* **2014**, *53*, 3229–3236. DOI: [10.1021/bi500421q](https://doi.org/10.1021/bi500421q).
- [58] Thomsen, R.; Christensen, M. H. MolDock: A New Technique for High-Accuracy Molecular Docking. *J. Med. Chem.* **2006**, *49*, 3315–3321. DOI: [10.1021/jm051197e](https://doi.org/10.1021/jm051197e).
- [59] LeadIT version 2.3.2; BioSolveIT GmbH, Sankt Augustin, Germany, **2017**, www.biosolveit.de/LeadIT.
- [60] Wolber, G.; Langer, T. LigandScout: 3D Pharmacophores Derived from Protein Bound Ligands and Their Use as Virtual Screening Filters. *J. Chem. Inf. Model.* **2005**, *45*, 160–169. DOI: [10.1021/ci049885e](https://doi.org/10.1021/ci049885e).
- [61] Kadam, R. U.; Roy, N. Recent Trends in Drug Likeness Prediction: A Comprehensive Review of *in Silico* Methods. *Indian J. Pharm. Sci.* **2007**, *69*, 609–615. DOI: [10.4103/0250-474X.38464](https://doi.org/10.4103/0250-474X.38464).
- [62] Lipinski, C. A.; Lombardo, F.; Dominy, B. W.; Feeney, P. J. Experimental and Computational Approaches to Estimate Solubility and Permeability in Drug Discovery and Development Settings. *Adv. Drug Deliv. Rev.* **2001**, *46*, 3–26. DOI: [10.1016/S0169-409X\(96\)00423-1](https://doi.org/10.1016/S0169-409X(96)00423-1).
- [63] <https://www.molinspiration.com/cgi-bin/properties>.
- [64] Veber, D. F.; Johnson, S. R.; Cheng, H. Y.; Smith, B. R.; Ward, K. W.; Kopple, K. D. Molecular Properties That Influence the Oral Bioavailability of Drug Candidates. *J. Med. Chem.* **2002**, *45*, 2615–2623. DOI: [10.1021/jm020017n](https://doi.org/10.1021/jm020017n).
- [65] <https://preadmet.bmdrc.kr/toxicity/>.
- [66] <https://molsoft.com/mprop/>.